I&EC research
Industrial & Engineering Chemistry Research

Article

pubs.acs.org/IECR

Modeling the Solubility of SO_2 + CO_2 Mixtures in Brine at Elevated Pressures and Temperatures

Sugata P. Tan,* Yao Yao, and Mohammad Piri

Department of Chemical and Petroleum Engineering, University of Wyoming, Laramie, Wyoming 82071, United States

Supporting Information

ABSTRACT: The knowledge of solubility behavior of SO_2 + CO_2 mixtures in brines at elevated pressures and temperatures is important both in the viability investigations of geologic cosequestrations into deep saline aquifers and in the simulations for flue gas sequestration. We present a model describing SO_2 and CO_2 as species that do not self-associate but cross associate with water. Two equations of state, PCSAFT/PMSA and eCPA, are applied to work with the model at conditions relevant to geologic sequestration of flue gases: up to 393 K and 450 bar (equivalent to a depth of 4 km) and high salt molality of 6. PC-SAFT/PMSA, which performs better in the whole range of interest, shows that the presence of SO_2 makes CO_2 less soluble in low-salinity brines (molality <1) but more soluble in high-salinity brines in a temperature range between the critical temperatures of the gases (31.1−157.5 °C).

INTRODUCTION

In designing geological sequestration of CO_2 in deep saline aquifers one needs to know the phase behavior of CO_2 and other impurities such as SO_x and NO_x in underground brines at elevated pressures and temperatures. SO_2 is a major impurity, particularly in flue gases generated from coal combustion, that exists in the amount of typically less than 0.5 wt % of CO_2.[1] Despite its small concentration, the presence of SO_2 will eventually influence the geochemistry of water−rock systems.[2−4] Therefore, the viability of the cosequestration of SO_2 + CO_2 mixtures in brines still needs further studies, in which the knowledge of mixture solubility in brines becomes very important. At the downstream of the cosequestration research, the viability will benefit coal-based power plants by eliminating the need of SO_2 scrubbers,[5] as the whole flue gas may be sequestered without advanced separation, and fee for the permit to emit SO_2.[6]

There have been studies on this cosequestration, but mostly concerned with the fate of these gases after they dissolve in brines.[2−4,7] Only a few studied the solubility, which is a crucial input for modeling the chemical reactions following the dissolution.[7,8] These studies were carried out in fresh water[8] and low-salinity brines (1 M NaCl)[7] using experimental approach and Henry's law, respectively. As far as the phase behavior is concerned, there is no experimental data for the mixture of SO_2 and CO_2 in brines due to its high corrosivity to the experimental setup. As an alternative to conducting the experiments, a thermodynamic equation of state (EOS) can be used to describe the phase behavior accurately as long as it is well tested and correctly validated. Once the EOS is set up, the investigation can be carried out over the whole range of pressure, temperature, salinity, and composition of interest. Furthermore, in a larger simulation scheme, the EOS may serve as a reliable module with flash-calculation tasks, which provide the main program with the equilibrium compositions of the phases.

There are two different ways to model the solubility of SO_2 and CO_2 in water. The first approach is to account for the speciation reactions of the gases with water, which involve bisulfite and sulfite ions for SO_2 in water,[9,10] and bicarbonate and carbonate ions for CO_2 in water.[11,12] The backbone of this approach is Pitzer's model,[13] which is unfortunately not easy to apply at once with two different gases due to its highly empirical nature. The second approach is to calculate the total amount of the gases dissolved in water, thus including the ionic forms resulting from the chemical reactions. The latter approach is attractive due to its simplicity and its straightforward interpretation for gas sequestration purposes. In this work, we apply the latter approach using a molecular EOS to model the corrosive system, thus providing the solubility behavior needed for the sequestration viability investigations and operational designs.

Whereas the phase behavior of CO_2 in brines has been rigorously studied experimentally and theoretically, the study on the case of SO_2 in brines is not as comprehensive. Numerous thermodynamic models have been applied to describe CO_2 in brines,[14−18] but not for SO_2 in brines. Recently, a model for CO_2, SO_2, and some other gases in brine was presented.[19] The EOS used in the model was based on the combination of Peng−Robinson (PR) cubic EOS and Henry's law. It is also worth noting that in the mentioned work, the solubility of gas mixtures was presented only in pure water.

Some recent models for CO_2 in water or brines apply a new class of EOS that is based on molecular statistical mechanics, i.e., the statistical associating fluid theory (SAFT).[20−24] This new class of EOS has been known to have high reliability and predictability due to its robust underlying theories. SAFT has been widely applied in petrochemical industries in the last two decades at various conditions and a wide range of chemical systems.[25] In this work, we apply the perturbed-chain statistical associating fluid theory (PC-SAFT) EOS[26] coupled with the

Received: June 3, 2013
Revised: July 5, 2013
Accepted: July 11, 2013
Published: July 11, 2013

dx.doi.org/10.1021/ie4017557 | *Ind. Eng. Chem. Res.* 2013, 52, 10864−10872

primitive mean spherical approximation (PMSA)[27] to handle the ionic interactions due to the presence of salt. PC-SAFT is well-known to be accurate in representing fluid phase equilibria over a wide range of neutral chemical species up to high pressures and temperatures.[25] The electrolyte version of PC-SAFT also exists, but it uses the modified Debye–Hückel approximation to account for the ions,[28] which is inaccurate for brines with high salinity. However, the combination of PC-SAFT and PMSA in this work enables the EOS to work at high salinity, which is important to deal with, for instance, situations close to the injection well. The new EOS version is referred to as PC-SAFT/PMSA. To the best of our knowledge, the model presented in this paper is the only one that handles CO_2 + SO_2 mixtures in brines with a salt concentration of up to 6 mols per kg water at elevated pressures and temperatures.

We also present the performance of another EOS that is a hybrid between a cubic EOS and the association framework of SAFT. In this work we use the electrolyte version of cubic plus association (eCPA),[29] which couples the popular Soave–Redlich–Kwong (SRK) cubic EOS with the association term (to handle the molecular association) and the PMSA (to handle the ionic interactions) similar to that used in the PCSAFT/PMSA. In previous studies, versions of cubic EOS were combined with electrostatic terms without applying the association,[30,31] which is important to describe water molecules better.

MODELING

We model the water molecule to consist of a single segment with two associating sites of proton-donor type and two associating sites of proton-acceptor type. The association between molecules, in this case also known as hydrogen bonding, occurs between two sites of different types. The proton-donor sites in water molecules belong to the hydrogen atoms, while the other type belong to the electron lone-pairs in the oxygen atoms. Therefore, four electron lone-pairs that are also present in the oxygen atoms of SO_2 and CO_2 contribute four associating sites of proton-acceptor type in each molecule. These sites enable the gases to cross associate with water molecules, but do not associate among themselves. For SO_2, there is an extra electron lone-pair in sulfur atom, which makes the total of five sites of proton-acceptor type. The presence of this extra site is consistent with the fact that SO_2 is more soluble in water than CO_2. Figure 1 shows the associating sites in H_2O, SO_2, and CO_2 in our model.

The ions are modeled as single segments that interact with one another through the hard-core and long-range Coulombic interactions. They also interact with the electrically neutral molecules (water and the gases) through the hard-core and dispersion interactions. In this work, the brine is assumed to contain only NaCl, which is the major salt dissolved in aquifers. This approximation is justified through investigative calculations,[32] from which it is known that the approximation introduces noticeable difference (at about 5%) only for the density at the highest salinity considered in this work.

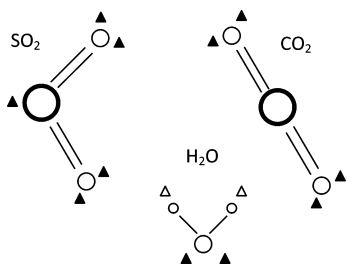

Figure 1. Association scheme of the molecules in our model; triangles are the associating sites (empty: proton-donor type; filled: proton-acceptor type).

In the following, we will briefly introduce the EOS that we use to apply the model for this particular system, i.e., PCSAFT/PMSA and eCPA. The details of both EOS can be found in the Supporting Information (SI) that accompanies this paper.

PCSAFT/PMSA. The EOS calculates the residual Helmholtz free energy of the chemical system, i.e., the gases + brine in our case, as follows.

$$\tilde{A}^{\mathrm{res}} = \tilde{A}^{\mathrm{hs}} + \tilde{A}^{\mathrm{chain}} + \tilde{A}^{\mathrm{disp}} + \tilde{A}^{\mathrm{assoc}} + \tilde{A}^{\mathrm{ion}} \quad (1)$$

where the superscripts of the free energy terms on the right-hand side of eq 1 are hard-sphere, chain, dispersion, association, and ion, respectively. These refer to the molecular interactions in the system: the hard-core repulsion, the chain-forming covalent bond, the van-der-Waals type of dispersive attraction, the highly directed associating interaction through hydrogen bonds, and the long-range electrostatic interactions between ions, respectively.

For each species in the system, the EOS has three parameters: the segment number m, the segment diameter σ, and the segment energy ε. For self-associating species, there are two additional parameters: the association volume κ and the association energy ε_A. For ions, we have another extra parameter, namely the hydrated diameter δ. The neutral species parameters are derived from the vapor–liquid equilibria (VLE) data, i.e., the vapor pressure and the saturated liquid density. The ionic parameters are derived from the mean activity coefficient ($\gamma_\pm$) data along with the density of the aqueous electrolytes (in our case, water + NaCl). Therefore, the ionic parameters are specific for aqueous solutions (water as the solvent). All PCSAFT/PMSA parameters are listed in Table 1. SO_2 and CO_2 do not self-associate, as indicated by their ε_A = 0, but cross associate with water molecules, as facilitated by their κ equal to that of water.[33]

eCPA. This EOS is the electrolyte version of the cubic plus association EOS,[34] which adds the association free energy term to a cubic EOS (PR[35] or SRK[29,36]) to describe systems with associating molecules. Without the association term, the cubic EOS does not perform well for such systems. The residual Helmholtz energy for the eCPA version[29,37] used in this paper is

$$\tilde{A}^{\mathrm{res}} = \tilde{A}^{\mathrm{SRK}} + \tilde{A}^{\mathrm{assoc}} + \tilde{A}^{\mathrm{PMSA}} + \tilde{A}^{\mathrm{Born}} \quad (2)$$

where the superscripts of the energy terms on the right-hand side are the SRK term from the original cubic EOS, the association term, and PMSA ionic term that are principally the same as in eq 1, and Born term that accounts for the ion transfer from a gas phase to a liquid solvent. Details of this EOS may be found elsewhere[38] and in the SI of this paper.

For each species, the eCPA has three parameters for the cubic SRK term: a_0, b, and c_1, in addition to the critical temperature (T_C is 647.1 K, 304.2 K, and 430.8 K for water, CO_2, and SO_2, respectively). For self-associating species, there are two additional parameters: the association volume κ and the association energy ε_A. For ions, additional information about their diameter σ is needed. The eCPA parameters for the species in our systems are listed in Table 2.

RESULTS AND DISCUSSION

In mixtures, where interactions between unlike species occur, binary interaction parameters k_{ij} are needed and derived from binary VLE data for interactions between neutral species, and

dx.doi.org/10.1021/ie4017557 | Ind. Eng. Chem. Res. 2013, 52, 10864–10872

Table 1. PCSAFT/PMSA Pure-Component and Ionic Parameters[a]

	m	σ (Å)	ε/k_B (K)[b]	associating sites[c]	ε_A/k_B (K)	κ
water	1.2190	eq5[d]	213.5741	(2,2)	1851.9773	0.052246
CO_2	2.0729	2.78520	169.2100	(0,4)	0	0.052246
SO_2	2.7566	2.71150	210.0274	(0,5)	0	0.052246
Na^+	1.0000	2.25183	eq6[d]	(0,0)		
Cl^-	1.0000	2.34298	eq7[d]	(0,0)		

[a]The ionic hydrated diameters are given in eqs 8 and 9. [b]k_B: Boltzmann constant. [c]First digit is the number of proton-donor type of associating sites; the second digit is the number of proton-acceptor type of associating sites. [d]Temperature-dependent functions as given in the corresponding equations.

Table 2. eCPA Pure-Component and Ionic Parameters

	a_0 (Pa·m^6/mol^2)	b ($\times 10^{-5}$ m^3/mol)	c_1	associating sites	ε_A/k_B (K)[c]	κ	σ ($\times 10^{-10}$ m)
water[a]	0.12277	1.45	0.6736	(2,2)	2003.248	0.0692	
CO_2[b]	0.35079	2.72	0.7602	(0,4)	0	0.0692	
SO_2	0.64621	3.52	0.8113	(0,5)	0	0.0692	
Na^+[d]	3.01600	1.04	0	(0,0)			3.21
Cl^-[d]	0.31500	1.99	0	(0,0)			3.98

[a]Ref 39. [b]Ref 40. [c]k_B: Boltzmann constant. [d]Ref 37, in which b is calculated from σ (see the SI).

Table 3. Coefficients of Binary Interaction Parameters in Eq 3

	PCSAFT/PMSA			eCPA		
binary	p	q	r	p	q	r
H_2O-CO_2	−0.41727	25.48	−3.2	−1.1996	70.624	−8.0
H_2O-SO_2	−0.00700			−0.3309	19.6727	−2.0629
H_2O-Na^+				0.5067	−74.695	13.494
H_2O-Cl^-				−0.3107	22.785	−4.3264
CO_2-SO_2	0.18204	−4.2143		0.1894	−3.33	
CO_2-Na^+	2.00721	−87.22	12.17	0.7123	−81.132	13.636
CO_2-Cl^-	2.00721	−87.22	12.17	0.7123	−81.132	13.636
SO_2-Na^+	−0.01272	6.25		1.6308	−134.34	21.25
SO_2-Cl^-	−0.01272	6.25		1.6308	−134.34	21.25
$k_{D\text{-}CO2}$[a]				8.4260	−530.66	68.182
$k_{D\text{-}SO2}$[a]				−3.9650	175.97	−31.250

[a]k_D is a fitted parameter in the expression of water dielectric constant to account for the presence of the gases; see the SI that accompanies this paper.

solubility data of the gases in brine for interactions involving ions. They are generally functions of temperature, i.e.,

$$k_{ij}(T) = p + q \times 10^{-4}T + r \times 10^{-6}T^2 \quad (3)$$

where the coefficients p, q, and r are listed in Table 3 for PCSAFT/PMSA and eCPA. The experimental data used to fit these parameters are listed in Table 4. The binary interaction parameters are used to correct the molecular interactions and implemented in the combining rule of the energy parameters:

Table 4. Experimental Data Used to Fit the Binary Interaction Parameters

binary	reference	temperature range	salt molality
H_2O-CO_2	Wiebe and Gaddy[41]	25−75 °C	
H_2O-SO_2	Rumpf and Maurer[9]	20−120 °C	
H_2O−NaCl	Pitzer et al.[42]	25−120 °C	up to 6
CO_2-SO_2	Cumming[43]	40−130 °C	
CO_2−NaCl in H_2O	Rumpf et al.[44]	40−120 °C	4 and 6
	Yan et al.[45]	50 °C	1 and 5
SO_2−NaCl in H_2O	Xia et al.[10]	40−120 °C	3

$$\varepsilon_{ij} = \sqrt{\varepsilon_i\varepsilon_j}(1 - k_{ij}) \quad \text{for PCSAFT/PMSA} \quad (4a)$$

$$\alpha_{ij} = \sqrt{\alpha_i\alpha_j}(1 - k_{ij}) \quad \text{for eCPA} \quad (4b)$$

The eCPA energy parameter α in eq 4b is related to the EOS parameters a_0 and c_1 (see the SI).

To improve the performance of PCSAFT/PMSA in aqueous electrolytes, the segment-diameter parameter of water was made temperature-dependent in representing the coexistence curve.[28] In this work, we refitted the parameter using a polynomial in reciprocal of temperature $(1/T)$ to get fewer coefficients but still obtain an equal performance. As the temperature changes from 25 to 120 °C, the water segment diameter varies from 2.8158 to 2.8247 Å. The temperature-dependent parameters, mostly of the ions, are listed in the following equations:

$$\sigma_1 = 2.798384 + 120.733275T^{-1} - 71515.85T^{-2} + 11052303T^{-3} \quad (\text{Å}) \quad (5)$$

$$\varepsilon^+/k_B = 798.7893(1 - 628.9294(T^{-1} - 298.15^{-1})) \quad (\text{K}) \quad (6)$$

dx.doi.org/10.1021/ie4017557 | Ind. Eng. Chem. Res. 2013, 52, 10864−10872

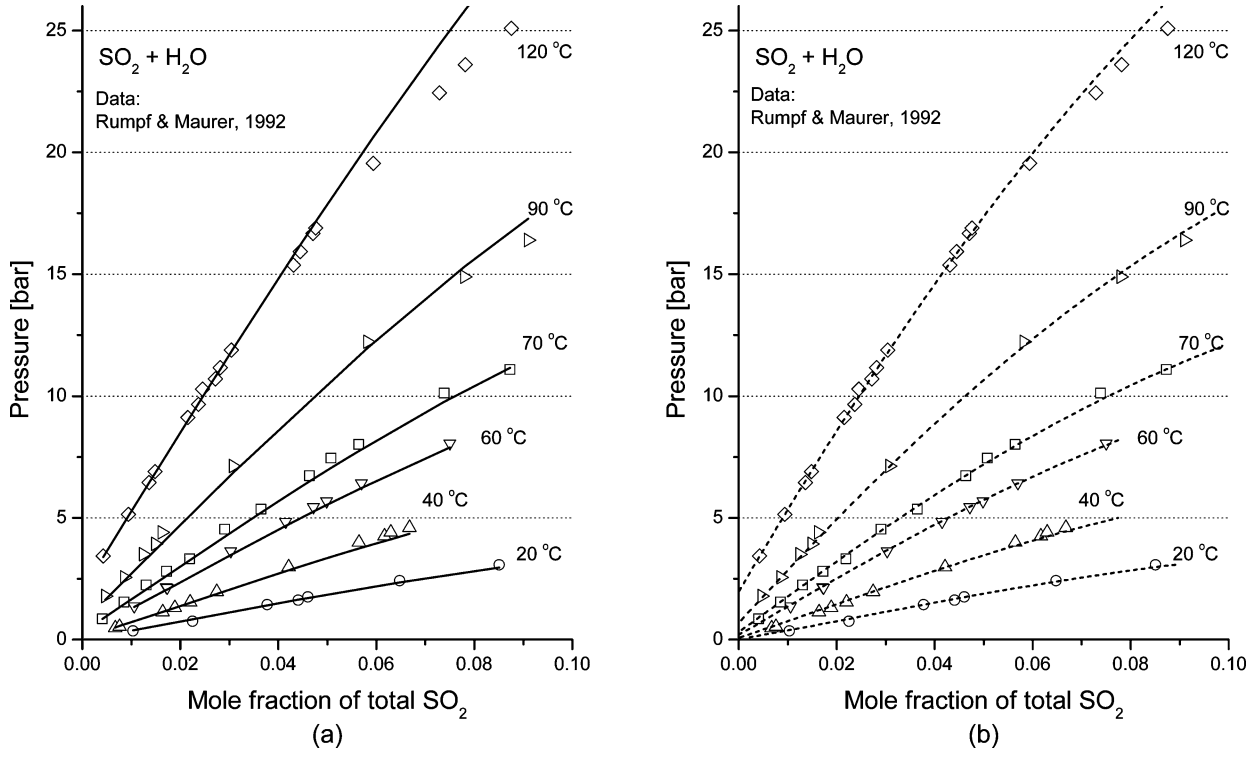

Figure 2. Fitted EOS for SO_2 dissolution in water: (a) PCSAFT and (b) CPA; symbols are experimental data.[9]

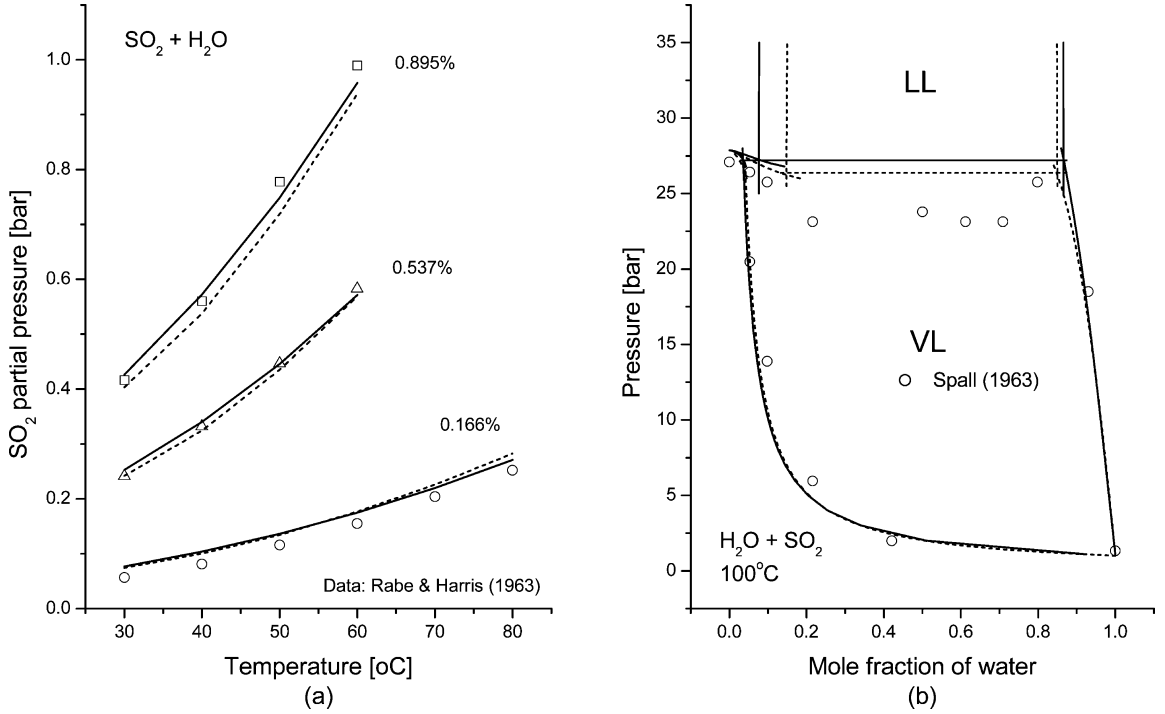

Figure 3. EOS predictions compared with other experimental data[46,47] for SO_2 dissolution in water: PCSAFT (solid curves) and CPA (dotted curves); percentages in panel a are mole fractions of SO_2; panel b also shows the existence of the second liquid phase.

$$\varepsilon^{-}/k_B = 112.2339(1 + 0.3644(T^{-1} - 298.15^{-1})) \quad \text{(K)} \tag{7}$$

$$\delta^{+} = 1.6470(1 - 1475.5590(T^{-1} - 298.15^{-1})) \quad \text{(Å)} \tag{8}$$

$$\delta^{-} = 8.2552(1 + 565.6977(T^{-1} - 298.15^{-1})) \quad \text{(Å)} \tag{9}$$

where the subscript 1 refers to water and the superscripts + and − refer to the positively and negatively charged ions, respectively (k_B is the Boltzmann constant).

On the other hand, as shown in Table 3, the eCPA applies binary parameters of ions with water to facilitate the temperature dependence upon relaxing the hard-sphere assumption of the ions. The binary parameters, however, are not unique, because

dx.doi.org/10.1021/ie4017557 | Ind. Eng. Chem. Res. 2013, 52, 10864−10872

the parameters of the individual ions are derived from the aqueous solution of the salt, not from pure ions. Therefore, in a strict sense, such derived ionic parameters have already contained some effects from water as the solvent. In this work, the binary parameters are still to appear in CPA to allow us to use the ionic parameters from the original eCPA work.[37] With this approach, we just extend the EOS application range to include higher temperatures and pressures using proper binary parameters.

To absorb the nonideality, the dielectric constant of water in eCPA is made a function of temperature and concentrations of both salt and the gas present in the brines; the latter is represented by gas-specific parameters, k_D, which are also included in Table 3. In contrast, the dielectric constant is just a function of temperature in PCSAFT/PMSA following its true values at different temperatures. See the SI for details.

Figures 2 and 3 show the EOS performance in SO_2 + water systems. The binary parameter was fitted to the VLE data[9] in Figure 2. This parameter was then used to calculate the phase diagrams in Figure 3 and then compared with experimental data,[46,47] which confirms that the model works with any concentrations of SO_2. It is worth noting that in Figure 2 eCPA applies a quadratic temperature-dependent binary parameter instead of a constant as PCSAFT does.

Figures 4 and 5 show the EOS performance for CO_2 + water systems, where the binary interaction parameter between CO_2

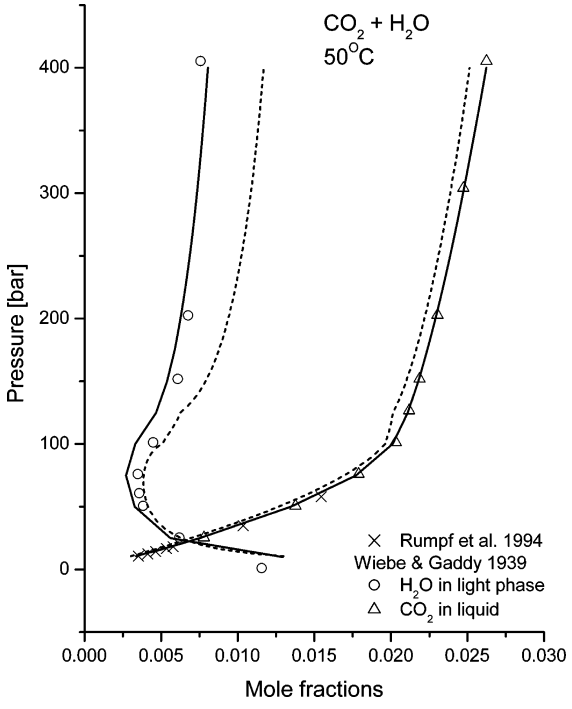

Figure 4. Fitted EOS for CO_2 dissolution in water: PCSAFT (solid curves) and CPA (dotted curve); symbols are experimental data.[41,44] The curves for mole fraction of water in the light phase are predictions (see text).

and water was derived from the VLE data[41,44] in Figure 4, where both EOS work equally well. However, the prediction using eCPA is slightly inaccurate at high pressures for the water content in the light phase, which is vapor at low pressures and CO_2-rich supercritical fluid phase at high pressures. Using this binary interaction, both EOS successfully predict the solubility curves in Figure 5 when compared with experimental data.[41,48−50] This

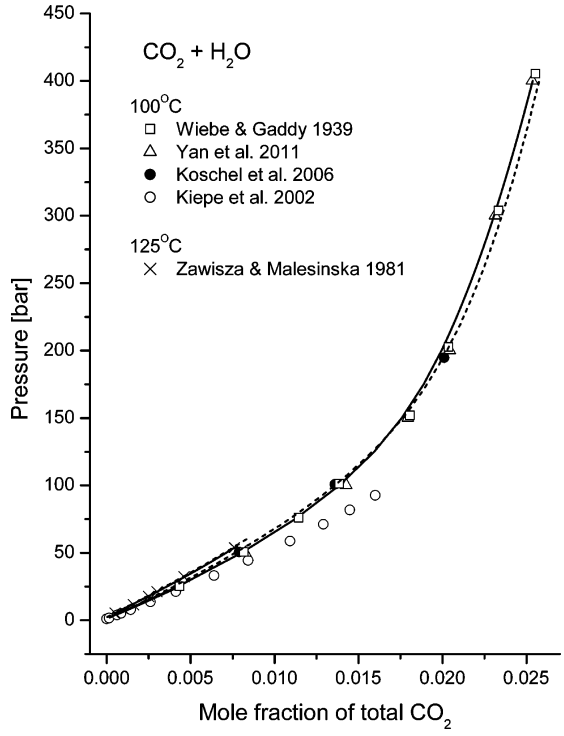

Figure 5. EOS predictions compared with other experimental data for CO_2 dissolution in water:[41−44] PCSAFT (solid curve) and CPA (dotted curve).

also confirms that they work at high temperatures. The solubility curves in the figures are the maximum amount of the gases at a particular pressure, temperature, and salinity, below which the gases can completely dissolve in the liquid phase.

Another important interaction parameter belongs to the mixture of CO_2 + SO_2, which was derived from the VLE data[43] of the binary system. The result is shown in Figure 6.

Based on the good performance that we obtained for all binary systems above, both EOS were employed, using all parameters in Tables 1−3, to describe the phase behavior of SO_2 in brine and CO_2 in brine; see Figures 7 and 8, respectively. The EOS performance in describing saline water, i.e., NaCl + water in this work, is provided in the SI.

We have a second liquid phase other than aqueous phase for SO_2 in brine at the high-pressure end of the solubility curves as shown in Figure 7. Because salt dissociations only occur in solvents with large dielectric constant, such as water, the salt is also assumed to stay in the aqueous phase when we have two liquids in equilibrium, as it is in the VLE case. Though both EOS overestimate the liquid−liquid regions at high temperatures, the deviation will not affect the EOS overall performance because the liquid−liquid region of this system lies at high SO_2 concentration, while our concern for SO_2 cosequestration is always at the lower concentration side.

In this work, we use solubility pressures to measure the degree of gas solubility. The solubility pressure is the total pressure, above which the whole amount of the gas dissolves in the solvent. Therefore, higher solubility pressure indicates lower solubility, such as that shown in Figure 7b, where the presence of salt increases the solubility pressure, which means it reduces the gas solubility. This phenomenon is known as the salting-out effect, which is also present in CO_2 + brine systems as shown in Figure 8.

dx.doi.org/10.1021/ie4017557 | Ind. Eng. Chem. Res. 2013, 52, 10864−10872

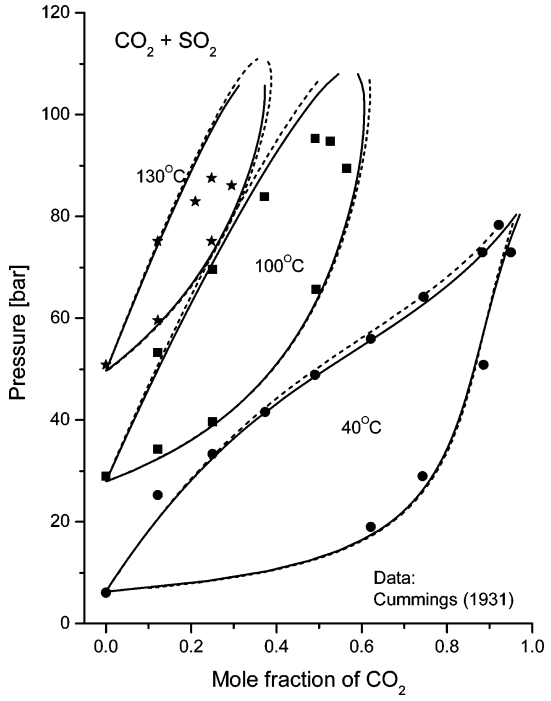

Figure 6. Fitted EOS calculation for the vapor–liquid equilibrium of CO_2 + SO_2 mixtures: PCSAFT (solid curves) and CPA (dotted curves); symbols are experimental data.[43]

For systems of CO_2 in brines shown in Figure 8, the supercritical phase is quite dominant at high pressures and at temperatures beyond the CO_2 critical temperature (31.1 °C). At a moderate temperature, for example, 50 °C, the supercritical phase appears above the points where the solubility pressure changes dramatically with the CO_2 concentration. At high temperatures, e.g., 100 °C, the curves are entirely in the supercritical region.

Evaluations on all of the results above, as evident from Figures 7 and 8, reveal that both EOS can be alternatives to each other except for high-salinity range at high pressures, where PCSAFT/PMSA substantially outperforms eCPA. This may be caused by the poorer performance of eCPA in describing the brines (see the SI). This fact in turn justifies the use of PCSAFT/PMSA to evaluate the phase behavior of SO_2 + CO_2 mixtures in brines in the whole range of temperature, pressure, and salinity of interest, for which experimental data are not available in the literature. This is the very idea of this work, i.e., using a reliable EOS to perform analyses on chemical systems that lack experimental data.

In sequestration schemes where the SO_2-to-CO_2 mole ratio is very small (in the order of 10^{-2}), the solubility curves will nearly coincide with those for CO_2 in Figure 8. Therefore, we calculate the phase diagrams at a much higher SO_2-to-CO_2 mole ratio (e.g., 2) in Figure 9 to discern the discrepancies. We use pressure–temperature phase diagrams, instead of pressure–concentration ones in Figures 7 and 8, to make the diagrams more useful for sequestration purposes as they can be superimposed with the underground pressure–temperature profiles of the geological sites.

In Figure 9a, the solubility curves of the gas mixture in brine are compared with those without SO_2. The solubility of CO_2 increases if the presence of SO_2 lowers the solubility pressure at a fixed temperature and gas composition. The solubility-pressure drop, or equivalently the solubility increase, is plotted against the temperature in Figure 9b to show the phase behavior more clearly. The pressure drop is the difference between the solubility pressure of the case with the presence of SO_2 and that with CO_2 only, i.e., the filled circles and the open circles in Figure 9a, respectively. The horizontal dotted line in the figure gives the

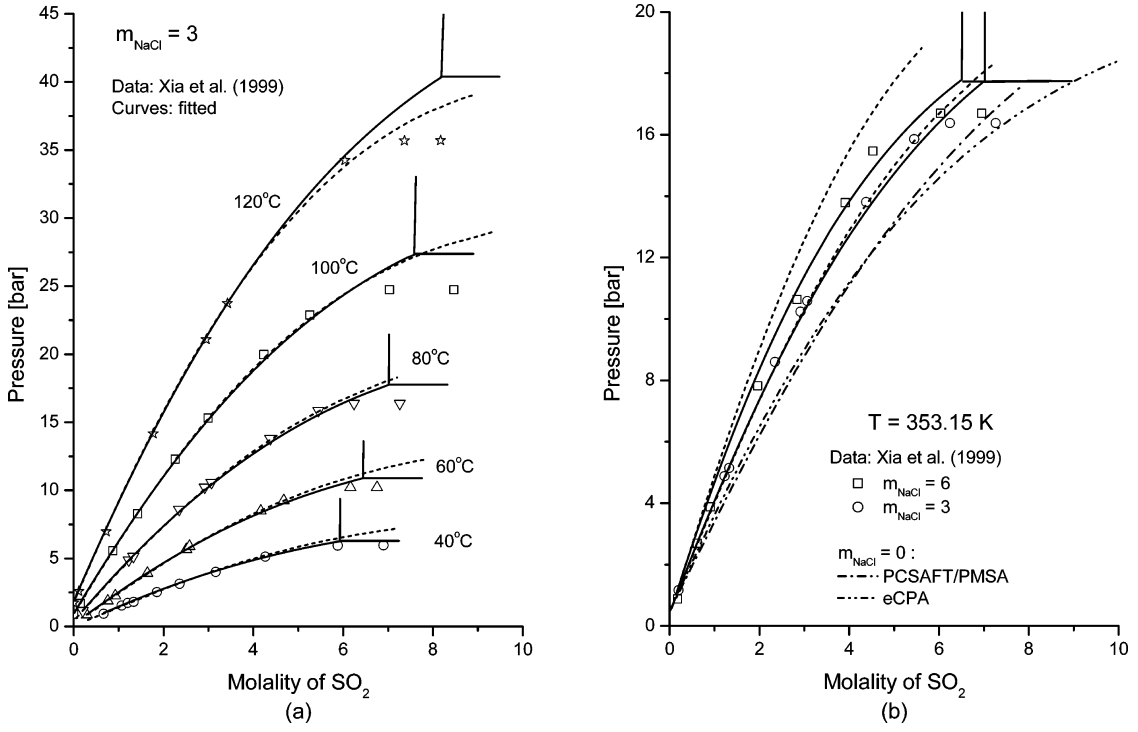

Figure 7. Solubility curves of SO_2 in brines: symbols are experimental data;[10] curves are calculated; the nearly vertical lines are calculated liquid–liquid equilibria (using PCSAFT/PMSA). The curves at the salt molality of 6 in panel b are predictions.

dx.doi.org/10.1021/ie4017557 | Ind. Eng. Chem. Res. 2013, 52, 10864–10872

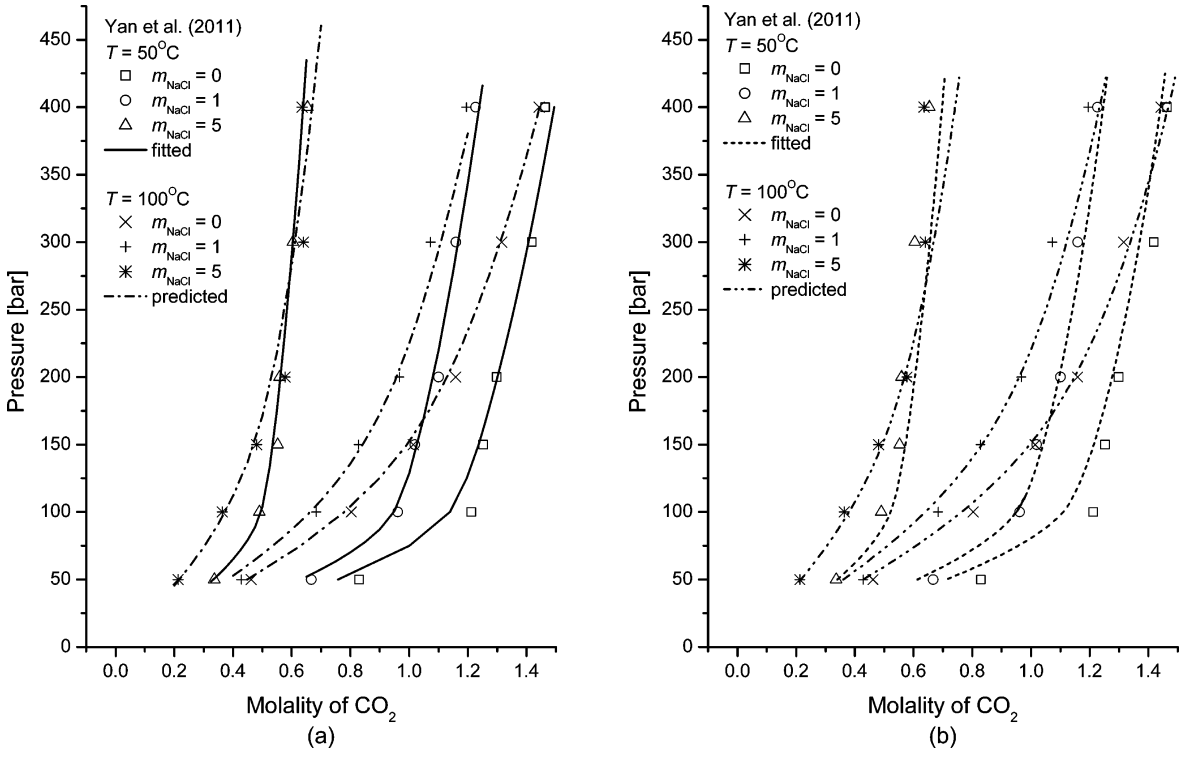

Figure 8. Solubility curves of CO_2 in brines: symbols are experimental data;[45] curves are calculated: (a) PCSAFT/PMSA and (b) eCPA.

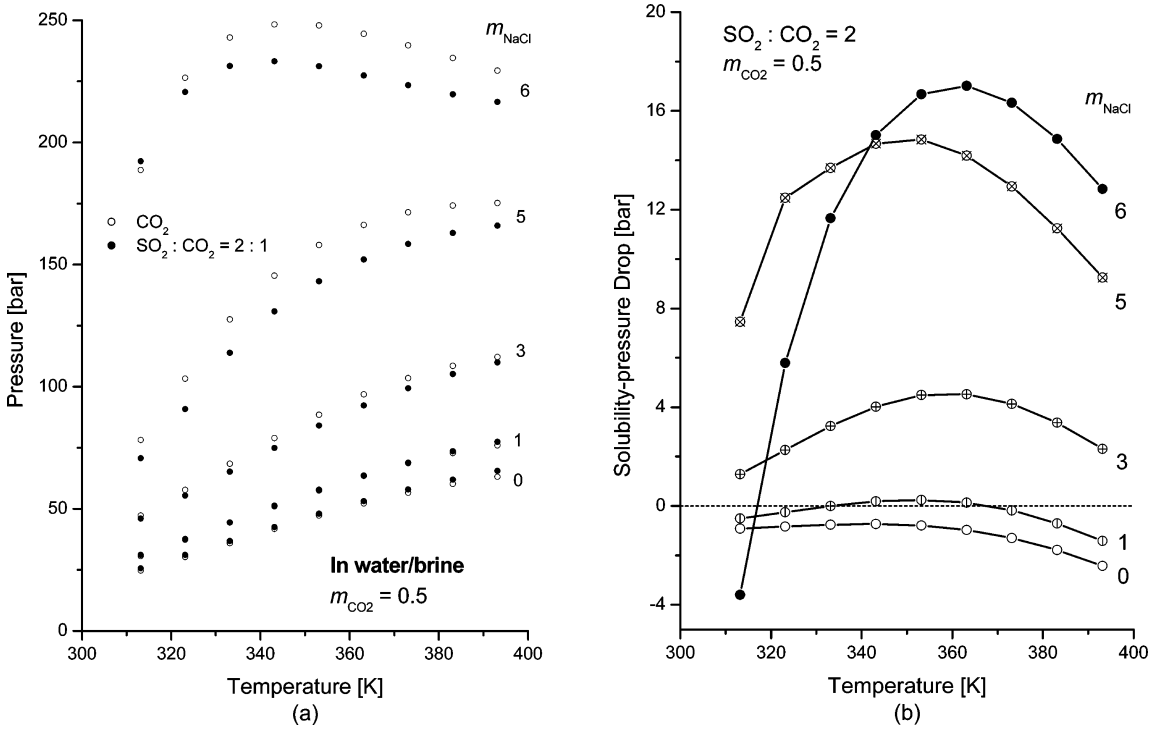

Figure 9. Phase behavior of $SO_2 + CO_2$ in brine at a SO_2-to-CO_2 mole ratio of 2 and a CO_2 molality of 0.5; symbols are calculated using PCSAFT/PMSA and lines are merely for visual guidance. The dotted line in panel b is when no SO_2 is present.

reference, i.e., the cases without SO_2, to which all pressure drops are calculated and referred. A positive pressure drop in Figure 9b means an increase in solubility, relative to that of the corresponding case without SO_2, at the same temperature and gas composition. Therefore, the presence of SO_2 increases the solubility of CO_2 in brines with salinities $m_{NaCl} > 1$ in the temperature range of 40 °C < T < 120 °C; at lower and higher temperatures the presence of SO_2 may decrease CO_2 solubility.

Similar to the plot in Figure 9b, Figure 10 shows the solubility-pressure drop if the SO_2-to-CO_2 mole ratio is reduced to 0.05, thus approaching the values in geologic cosequestration scenarios. Comparing the two figures, which differ only in the

dx.doi.org/10.1021/ie4017557 | Ind. Eng. Chem. Res. 2013, 52, 10864−10872

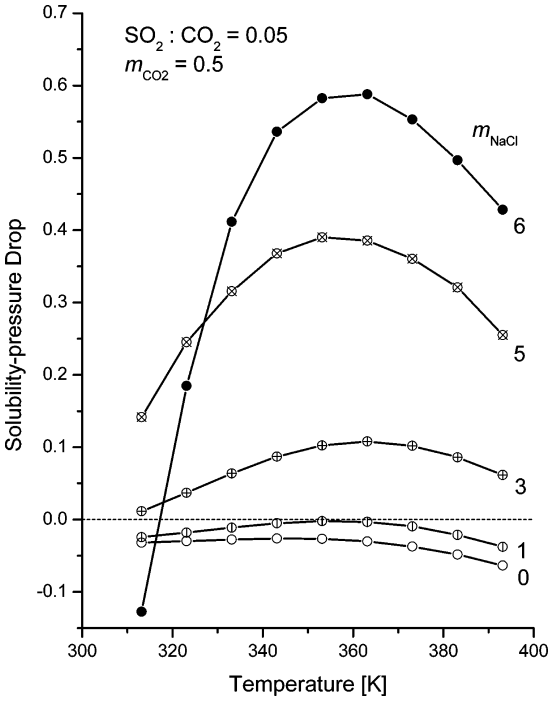

Figure 10. Phase behavior of SO_2/CO_2 in brine at a SO_2-to-CO_2 mole ratio of 0.05 and a CO_2 molality of 0.5; symbols are calculated using PCSAFT/PMSA; lines are for visual guidance.

amount of SO_2 impurity, concludes that the phase behaviors are qualitatively very similar to each other.

It is also evident from Figure 10 that in high-salinity brines, where the solubility of CO_2 (without SO_2) decreases due to the salting-out effect as was shown in Figure 8, the presence of SO_2 improves the solubility of CO_2 significantly. However, considering that the curve for $m_{NaCl} = 1$ lies in negative region at all temperatures, the SO_2 impurity makes CO_2 less soluble if the brine is of low salinity ($m_{NaCl} < 1$). Lower solubility can also be interpreted as higher total pressure that is required to get the whole gas mixture dissolved in the brine, which immediately translates to higher operating costs.

For the reservoir simulation studies of $SO_2 + CO_2$ cosequestration, one will need to note that at temperature range between the critical temperature of CO_2 (31.1 °C) and that of SO_2 (157.5 °C), where the relative solubility of the gas mixture increases, the higher solubility of the gases would enhance the chemical reactions that may occur between the generated ions and the geological minerals. This will indirectly affect the permanent storage of carbon dioxide.

CONCLUSIONS

The model in this work can describe the important chemical system of $SO_2 + CO_2$ + brine, the experimental data of which are absent in the literature, for flue gas sequestration. It can be used as a stand-alone solubility evaluator or as a module of a larger geologic sequestration simulation platform.

For the EOS to apply the model, PCSAFT/PMSA and eCPA may be alternatives to each other except for the high-salinity range at high pressures, where PCSAFT/PMSA substantially outperforms eCPA.

ASSOCIATED CONTENT

Supporting Information

Details of the EOS used in this work and the EOS performance in describing the properties of aqueous NaCl solutions. This material is available free of charge via the Internet at http://pubs.acs.org.

AUTHOR INFORMATION

Corresponding Author

*E-mail: sptan@uwyo.edu.

Notes

The authors declare no competing financial interest.

ACKNOWLEDGMENTS

This work is supported by DOE Financial Assistance Agreement DE-FE0004832, with M.P. as the PI. The financial support of the School of Energy Resources of the University of Wyoming is also acknowledged.

REFERENCES

(1) Miller, P. J.; Van Atten, C. *North American Power Plant Emissions*; Commission for Environmental Cooperation of North America: Montréal, Canada, 2004.

(2) Kaszuba, J. P.; Navarre-Sitchler, A.; Thyne, G.; Chopping, C.; Meuzelaar, T. Supercritical carbon dioxide and sulfur in the Madison Limestone: A natural analog in southwest Wyoming for geologic carbon−sulfur co-sequestration. *Earth Planet. Sci. Lett.* **2011**, *309*, 131−140.

(3) Glezakou, V.-A.; McGrail, B. P.; Schaef, H. T. Molecular interactions of SO_2 with carbonate minerals under co-sequestration conditions: A combined experimental and theoretical study. *Geochim. Cosmochim. Acta* **2012**, *92*, 265−274.

(4) Kummerow, J.; Spangenberg, E. Experimental evaluation of the impact of the interactions of CO_2-SO_2, brine, and reservoir rock on petrophysical properties: A case study from the Ketzin test site, Germany. *Geochem., Geophys., Geosyst.* **2011**, *12*, 10 DOI: 10.1029/2010GC003469.

(5) Woods, M. C.; Capicotto, P. J.; Haslbeck, J. L.; Kuehn, N. J.; Matuszewski, M.; Pinkerton, L. L.; Rutkowski, M. D.; Schoff, R. L.; Vaysman, V. *Cost and Performance Baseline for Fossil Energy Plants. Vol. 1: Bituminous Coal and Natural Gas to Electricity*; National Energy Technology Laboratory: Pittsburgh, PA, 2007.

(6) U.S. Environmental Protection Agency. *Acid Rain and Related Programs 2007 Progress Report*; EPA: Washington, DC, 2009.

(7) Crandell, L. E.; Ellis, B. R.; Peters, C. A. Dissolution potential of SO_2 co-injected with CO_2 in geologic sequestration. *Environ. Sci. Technol.* **2010**, *44*, 349−355.

(8) Sayegh, S. G.; Najman, J. Phase behavior measurements of CO_2-SO_2-brine mixtures. *Can. J. Chem. Eng.* **1987**, *65*, 314−320.

(9) Rumpf, B.; Maurer, G. Solubilities of hydrogen cyanide and sulfur dioxide in water at temperatures from 293.15 to 413.15 K and pressures up to 2.5 MPa. *Fluid Phase Equilib.* **1992**, *81*, 241−260.

(10) Xia, J.; Rumpf, B.; Maurer, G. The solubility of sulfur dioxide in aqueous solutions of sodium chloride and ammonium chloride in the temperature range from 313 to 393 K at pressures up to 3.7 MPa: Experimental results and comparison with correlations. *Fluid Phase Equilib.* **1999**, *165*, 99−119.

(11) Li, D.; Duan, Z. The speciation equilibrium coupling with phase equilibrium in the H_2O−CO_2−NaCl system from 0 to 250 °C, from 0 to 1000 bar, and from 0 to 5 molality of NaCl. *Chem. Geol.* **2007**, *244*, 730−751.

(12) Dickson A. G., Goyet, C., Eds. *Handbook of Methods for the Analysis of the Various Parameters of Carbon Dioxide System in Sea Water*, version 2; ORNL/CDIAC-74; U.S. Department of Energy, Oak Ridge National Laboratory: Oak Ridge, TN, 1994.

(13) Pitzer, K. S. Thermodynamics of electrolytes. I. Theoretical basis and general equations. *J. Phys. Chem.* **1973**, *77*, 268−277.
(14) Akinfiev, N. N.; Diamond, L. W. Thermodynamic model of aqueous CO_2−H_2O−NaCl solutions from −22 to 100 °C and from 0.1 to 100 MPa. *Fluid Phase Equilib.* **2010**, *295*, 104−124 and the references therein.
(15) Ji, Y.; Ji, X.; Feng, X.; Liu, C.; Lü, L.; Lu, X. Progress in the study on the phase equilibria of the CO_2-H_2O and CO_2-H_2O-NaCl systems. *Chin. J. Chem. Eng.* **2007**, *15*, 439−448 and the references therein.
(16) Duan, Z.; Møller, N.; Weare, J. H. Equation of state for the NaCl-H_2O-CO_2 system: Prediction of phase equilibria and volumetric properties. *Geochim. Cosmochim. Acta* **1995**, *59*, 2869−2882.
(17) Duan, Z.; Sun, R. An improved model calculating CO_2 solubility in pure water and aqueous NaCl solutions from 273 to 533 K and from 0 to 2000 bar. *Chem. Geol.* **2003**, *193*, 257−271.
(18) Harvey, A. H.; Prausnitz, J. M. Thermodynamics of high-pressure aqueous systems containing gases and salts. *AIChE J.* **1989**, *35*, 635−644.
(19) Ziabakhsh-Ganji, Z.; Kooi, H. An equation of state for thermodynamic equilibrium of gas mixtures and brines to allow simulation of the effects of impurities in subsurface CO_2 storage. *Int. J. Greenhouse Gas Control* **2012**, *11S*, S21−S34.
(20) Ji, X.; Tan, S. P.; Adidharma, H.; Radosz, M. SAFT1-RPM approximation extended to phase equilibria and densities of CO_2-H_2O and CO_2-H_2O-NaCl systems. *Ind. Eng. Chem. Res.* **2005**, *44*, 8419−8427.
(21) Tang, X.; Gross, J. Modeling the phase equilibria of hydrogen sulfide and carbon dioxide in mixture with hydrocarbons and water using the PCP-SAFT equation of state. *Fluid Phase Equilib.* **2010**, *293*, 11−21.
(22) Sun, R.; Dubessy, J. Prediction of vapor−liquid equilibrium and PVTx properties of geological fluid system with SAFT-LJ EOS including multi-polar contribution. Part II: Application to H_2O−NaCl and CO_2−H_2O−NaCl system. *Geochim. Cosmochim. Acta* **2012**, *88*, 130−145.
(23) Islam, A. W.; Carlson, E. S. Application of SAFT equation for CO_2 + H_2O phase equilibrium calculations over a wide temperature and pressure range. *Fluid Phase Equilib.* **2012**, *321*, 17−24.
(24) Diamantonis, N. I.; Economou, I. G. Modeling the phase equilibria of a H_2O−CO_2 mixture with PC-SAFT and tPC-PSAFT equations of state. *Mol. Phys.* **2012**, *110*, 1205−1212.
(25) Tan, S. P.; Adidharma, H.; Radosz, M. Recent advances and applications of statistical associating fluid theory. *Ind. Eng. Chem. Res.* **2008**, *47*, 8063−8082.
(26) Gross, J.; Sadowski, G. Perturbed-Chain SAFT: An equation of state based on a perturbation theory for chain molecules. *Ind. Eng. Chem. Res.* **2001**, *40*, 1244−1260.
(27) Blum, L.; Høye, J. S. Mean spherical model for asymmetric electrolytes. 2. Thermodynamic properties and the pair correlation function. *J. Phys. Chem.* **1977**, *81*, 1311.
(28) Held, C.; Cameretti, L. F.; Sadowski, G. Modeling aqueous electrolyte solutions. Part 1. Fully dissociated electrolytes. *Fluid Phase Equilib.* **2008**, *270*, 87−96.
(29) Inchekel, R.; de Hemptinne, J.-C.; Fürst, W. The simultaneous representation of dielectric constant, volume and activity coefficients using an electrolyte equation of state. *Fluid Phase Equilib.* **2008**, *271*, 19−27.
(30) Aasberg-Petersen, K.; Stenby, E.; Fredenslund, A. Prediction of high-pressure gas solubilities in aqueous mixtures of electrolytes. *Ind. Eng. Chem. Res.* **1991**, *30*, 2180−2185.
(31) Zuo, Y.-X.; Guo, T.-M. Extension of the Patel-Teja equation of state to the prediction of the solubility of natural gas in formation water. *Chem. Eng. Sci.* **1991**, *46*, 3251−3258.
(32) Ji, X.; Tan, S. P.; Adidharma, H.; Radosz, M. Statistical associating fluid theory coupled with restricted primitive model extended to bivalent ions. SAFT2: 2. Brine/seawater properties predicted. *J. Phys. Chem. B* **2006**, *110*, 16700−16706.
(33) Kleiner, M.; Sadowski, G. Modeling of polar systems using PCP-SAFT: An approach to account for induced-association interactions. *J. Phys. Chem. C.* **2007**, *111*, 15544−15553.
(34) Kontogeorgis, G. M.; Voutsas, E. C.; Yakoumis, I. V.; Tassios, D. P. An equation of state for associating fluids. *Ind. Eng. Chem. Res.* **1996**, *35*, 4310−4318.
(35) Wu, J.; Prausnitz, J. M. Phase equilibrium for systems containing hydrocarbons, water and salt: An extended Peng-Robinson equation of state. *Ind. Eng. Chem. Res.* **1998**, *37*, 1634−1643.
(36) Lin, Y.; Thomsen, K.; de Hemptinne, J.-C. Multicomponent equations of state for electrolytes. *AIChE J.* **2007**, *53*, 989−1005.
(37) Inchekel, R. *Développement d'une équation d'état applicable aux systèmes d'électrolytes eau-alcool-sels-hydrocarbures*. Dissertation, Mines Paris Tech, 2008, Table 25 (p 117).
(38) Kontogeorgis, G. M.; Folas, G. K. *Thermodynamic Models for Industrial Applications: From Classical and Advanced Mixing Rules to Association Theories*; John Wiley & Sons, Ltd.: Chichester, U.K., 2010.
(39) Folas, G. K.; Kontogeorgis, G. M.; Michelsen, M. L.; Stenby, E. H. Application of the cubic-plus-association equation of state to mixtures with polar chemicals and high pressures. *Ind. Eng. Chem. Res.* **2006**, *45*, 1516−1526.
(40) Tsivintzelis, I.; Kontogeorgis, G. M.; Michelsen, M. L.; Stenby, E. H. Modeling phase equilibria for acid gas mixtures using the CPA equation of state. Part II: Binary mixtures with CO_2. *Fluid Phase Equilib.* **2011**, *306*, 38−56.
(41) Wiebe, R.; Gaddy, V. L. The solubility in water of carbon dioxide at 50, 75 and 100°, at pressures to 700 atm. *J. Am. Chem. Soc.* **1939**, *61*, 315−318.
(42) Pitzer, K. S.; Peiper, J. C.; Busey, R. H. Thermodynamic properties of aqueous sodium chloride solutions. *J. Phys. Chem. Ref. Data* **1984**, *13*, 1−102.
(43) Cummings, L. W. T. High-pressure rectification. I- Vapor-liquid equilibrium relations at high pressures. *Ind. Eng. Chem.* **1931**, *23*, 900−902.
(44) Rumpf, B.; Nicolaisen, H.; Ocal, C.; Maurer, G. Solubility of carbon dioxide in aqueous solutions of sodium chloride: Experimental results and correlation. *J. Solution Chem.* **1994**, *23*, 431−448.
(45) Yan, W.; Huang, S.; Stenby, E. H. Measurement and modeling of CO_2 solubility in NaCl brine and CO_2−saturated NaCl brine density. *Int. J. Greenhouse Gas Control* **2011**, *5*, 1460−1477.
(46) Rabe, A. E.; Harris, J. F. Vapor liquid equilibrium data for the binary system, sulfur dioxide and water. *J. Chem. Eng. Data* **1963**, *8*, 333−336.
(47) Spall, B. C. Phase equilibria in the system sulphur dioxide-water from 25−300 C. *Can. J. Chem. Eng.* **1963**, *41*, 79−83.
(48) Koschel, D.; Coxam, J.-Y.; Rodier, L.; Majer, V. Enthalpy and solubility data of CO_2 in water and NaCl(aq) at conditions of interest for geological sequestration. *Fluid Phase Equilib.* **2006**, *247*, 107−120.
(49) Kiepe, J.; Horstmann, S.; Fischer, K.; Gmehling, J. Experimental determination and prediction of gas solubility data for CO_2 + H_2O mixtures containing NaCl or KCl at temperatures between 313 and 393 K and pressures up to 10 MPa. *Ind. Eng. Chem. Res.* **2002**, *41*, 4393−4398.
(50) Zawisza, A.; Malesinska, B. Solubility of carbon dioxide in liquid water and of water in gaseous carbon dioxide in the range 0.2−5 MPa and at temperatures up to 473 K. *J. Chem. Eng. Data* **1981**, *26*, 388−391.